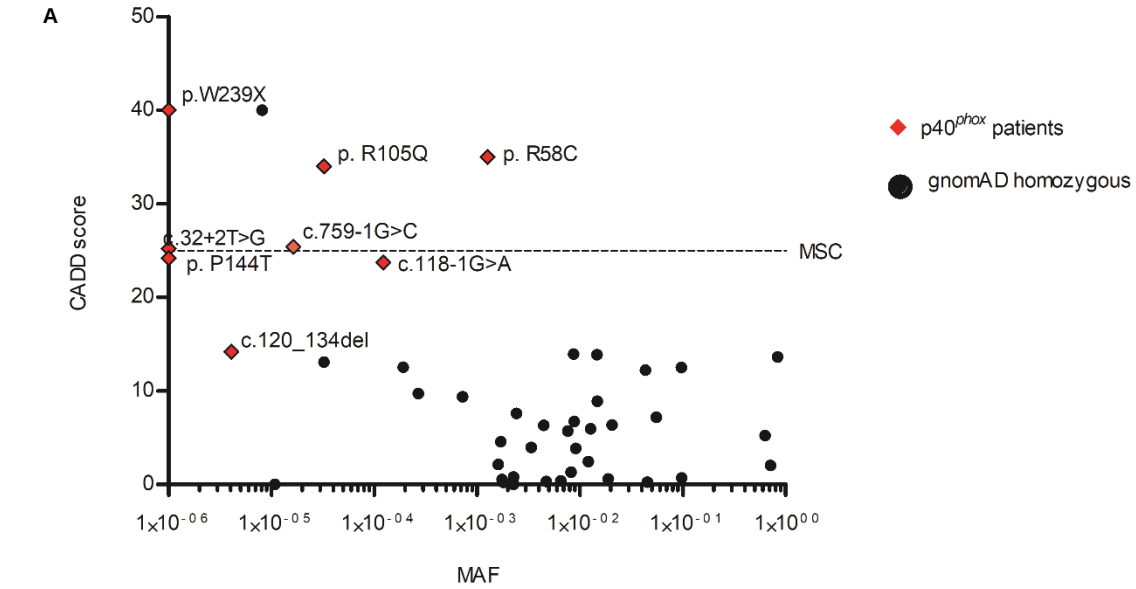

B

	R58C	R105Q	P144T
Homo sapiens	GGSKYLIYRRYRQFHALQSK	GVKQEIAEMRIPALNAYMK	QSPYDSEQVPQALRRLRPRT
Colobus angolensis palliatus	GGSKYLIYRRYRQFHALQSK	GVKQEIAEMRIPALNAYMK	QSPYDSEQVPQALRRLRPRT
Chlorocebus sabaeus	GGSKYLIYRRYRQFHALQSK	GVKQEIAEMRIPALNAYMK	QSPYDSEQVPQALRRLRPRT
Rhinopithecus bieti	GGSKYLIYRRYRQFHALQSK	GVKQEIAEMRIPALNAYMK	QSPYDSEQVPQALRRLRPRT
Saimiri boliviensis	GGSKYLIYRRYRQFHALQSK	GVKQEIAEMRIPALNAYMK	QSPYDSEQVPQALRRLRPRT
boliviensis	GGSKYLIYRRYRQFHALQSK	GVKQEIAEMRIPALNAYMK	QSPYDSEQVPQALRRLRPRT
Pan paniscus	GGSKYLIYRRYRQFHALQSK	GVKQEIAEMRIPALNAYMK	QSPYDSEQVPQALRRLRPRT
Otolemur garnettii	GGSKYLIYRRYRQFHALQSK	GVKQEIAEMRIPALNAYMK	QSPYDSEQVPQALRRLRPRT
Cebus capucinus imitator	GGSKYLIYRRYRQFHALQSK	GVKQEIAEMRIPALNAYMK	QSPYDSEQVPQALRRLRPRT
Pan troglodytes	GGSKYLIYRRYRQFHALQSK	GVKQEIAEMRIPALNAYMK	QSPYDSEQVPQALRRLRPRT
Propithecus coquereli	GGSKYLIYRRYRQFHALQSK	GVKQEIAEMRIPALNAYMK	QSPYDSEQVPQALRRLRPRT
Macaca fascicularis	GGSKYLIYRRYRQFHALQSK	GVKQEIAEMRIPALNAYMK	QSPYDSEQVPQALRRLRPRT
Mandrillus leucophaeus	GGSKYLIYRRYRQFHALQSK	GVKQEIAEMRIPALNAYMK	QSPYDSEQVPQALRRLRPRT
Nomascus leucogenys	GGSKYLIYRRYRQFHALQSK	GVKQEIAEMRIPALNAYMK	QSPYDSEQVPQALRRLRPRT
Rhinopithecus roxellana	GGSKYLIYRRYRQFHALQSK	GVKQEIAEMRIPALNAYMK	QSPYDSEQVPQALRRLRPRT
Gorilla gorilla gorilla	GGSKYLIYRRYRQFHALQSK	GVKQEIAEMRIPALNAYMK	QSPYDSEQVPQALRRLRPRT
Aotus nancymaae	GGSKYLIYRRYRQFHALQSK	GVKQEIAEMRIPALNAYMK	QSPYDSEQVPQALRRLRPRT
Macaca mulata	GGSKYLIYRRYRQFHALQSK	GVKQEIAEMRIPALNAYMK	QSPYDSEQVPQALRRLRPRT
Callithrix jacchus	GGSKYLIYRRYRQFHALQSK	GVKQEIAEMRIPALNAYMK	QSPYDSEQVPQALRRLRPRT
Microcebus murinus	GGSKYLIYRRYRQFHALQSK	GVKQEIAEMRIPALNAYMK	QSPYDSEQVPQALRRLRPRT
Papio anubis	GGSKYLIYRRYRQFHALQSK	GVKQEIAEMRIPALNAYMK	QSPYDSEQVPQALRRLRPRT
Pongo abelii	GGSKYLIYRRYRQFHALQSK	GVKQEIAEMRIPALNAYMK	QSPYDSEQVPQALRRLRPRT
Macaca nemestrina	GGSKYLIYRRYRQFHALQSK	GVKQEIAEMRIPALNAYMK	QSPYDSEQVPQALRRLRPRT
Cercocebus atys	GGSKYLIYRRYRQFHALQSK	GVKQEIAEMRIPALNAYMK	QSPYDSEQVPQALRRLRPRT
Carlito syrichta	GGSKYLIYRRYRQFHALQSK	GVKQEIAEMRIPALNAYMK	QSPYDSEQVPQALRRLRPRT
Chlorocebus sabaeus	*GGSKYLIYRRYRQFYALQSK*	GVKQEIAEMRIPALNAYMK	QSPYDSEQVPQALRRLRPRT
Rattus norvegicus	*GGSKYLIYRRYRQFYALQSK*	GVKQEIAETRIPALNAYMK	QSAYDAEQVPQALRRLRPRT
Mus musculus	*GGSKYLIYRRYRQFYALQSK*	GAKQEIAETRIPALNAYMK	QSAYDAEQVPQALRRLRPRT
Canis familiaris	*GGSKYLIYRRYRQFHALQSK*	GVKQEIAEMRIPALNAYMK	QSPYDSEQVPQALRRLRPRT
Bos taurus	*GGSKYLIYRRYRQFYALQSK*	GVKQEIAEMRIPALNAYMK	QSSYDAEQVPQALRRLRPRT
Ornithorhynchus anatinus	*GGSRYLIYRRYSQFYALHTK*	GVKQEIAENRIPALNCYMK	QSSYDAEQVPQGLRRLRPRT
Gallus gallus	*SGGRYLIFRRYREFYALHTK*	GAKREIAENRIPILNIYMK	HSIFDSEQVPRRLRSLRPRL
Xenopus tropicalis	*GSSKYFIYRRYSQFFTLHAK*	GNKKDIAETRIPLLNGYMK	QTLSDSEGIPRALRRLRPQT
Saccaromyces cerevisiae	*RNHKKLDLDRHLNTYNKHEK*	TLYNRLQDMKIPYLNSDIV	KLGYSKAKLEMTRRKYGVAT

Supplementary figure 1.

Identification of *NCF4* mutations. **(A)** All homozygous variants of *NCF4* present in gnomAD are plotted according to their CADD scores (*y*-axis) and minor allele frequency (MAF, *x*-axis). Red diamonds correspond to the mutations found in the 24 patients of this study. The dashed line indicates the mutation significance cutoff MSC. **(B)** Amino-acid residue conservation for the three missense mutations found in kindreds B, G, H and L.

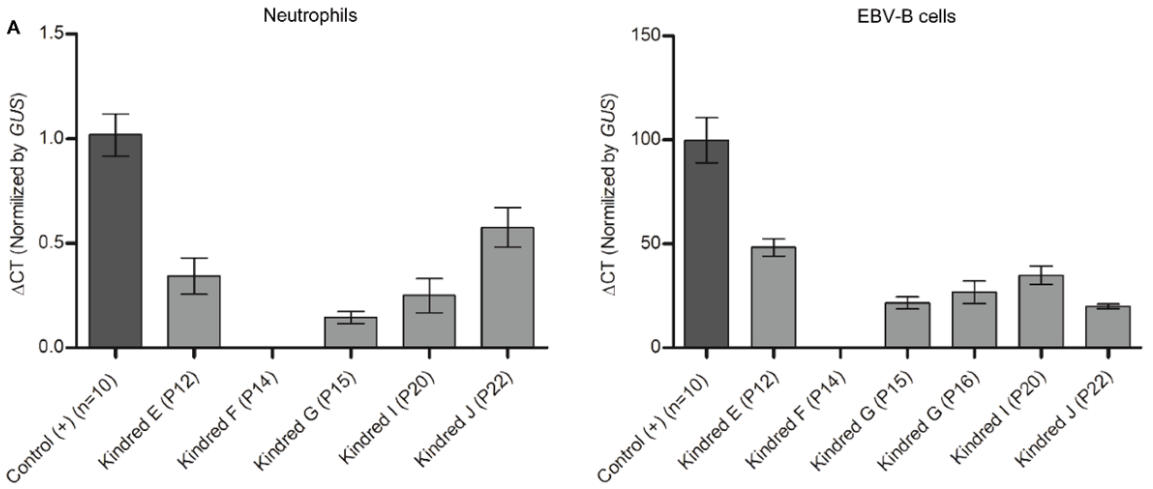
A
Neutrophils
ΔCT (Normalized by GUS)
1.5
1.0
0.5
0.0
Control (+) (n=10)
Kindred E (P12)
Kindred F (P14)
Kindred G (P15)
Kindred I (P20)
Kindred J (P22)
EBV-B cells
150
100
50
0
Control (+) (n=10)
Kindred E (P12)
Kindred F (P14)
Kindred G (P15)
Kindred G (P16)
Kindred I (P20)
Kindred J (P22)

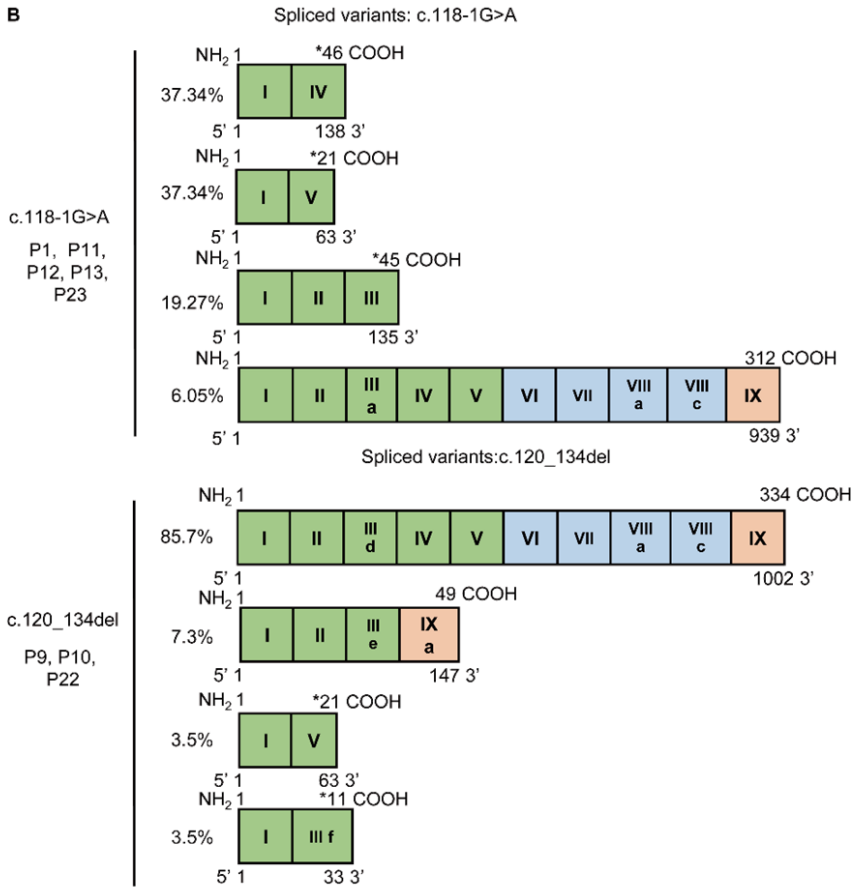
B
Spliced variants: c.118-1G>A
c.118-1G>A
P1, P11, P12, P13, P23
NH2 1
*46 COOH
37.34%
I IV
5' 1
138 3'
NH2 1
*21 COOH
37.34%
I V
5' 1
63 3'
NH2 1
*45 COOH
19.27%
I II III
5' 1
135 3'
NH2 1
312 COOH
6.05%
I II III a IV V VI VII VIII a VIII c IX
5' 1
939 3'
Spliced variants:c.120_134del
c.120_134del
P9, P10, P22
NH2 1
334 COOH
85.7%
I II III d IV V VI VII VIII a VIII c IX
5' 1
1002 3'
NH2 1
49 COOH
7.3%
I II III e IX a
5' 1
147 3'
NH2 1
*21 COOH
3.5%
I V
5' 1
63 3'
NH2 1
*11 COOH
3.5%
I III f
5' 1
33 3'

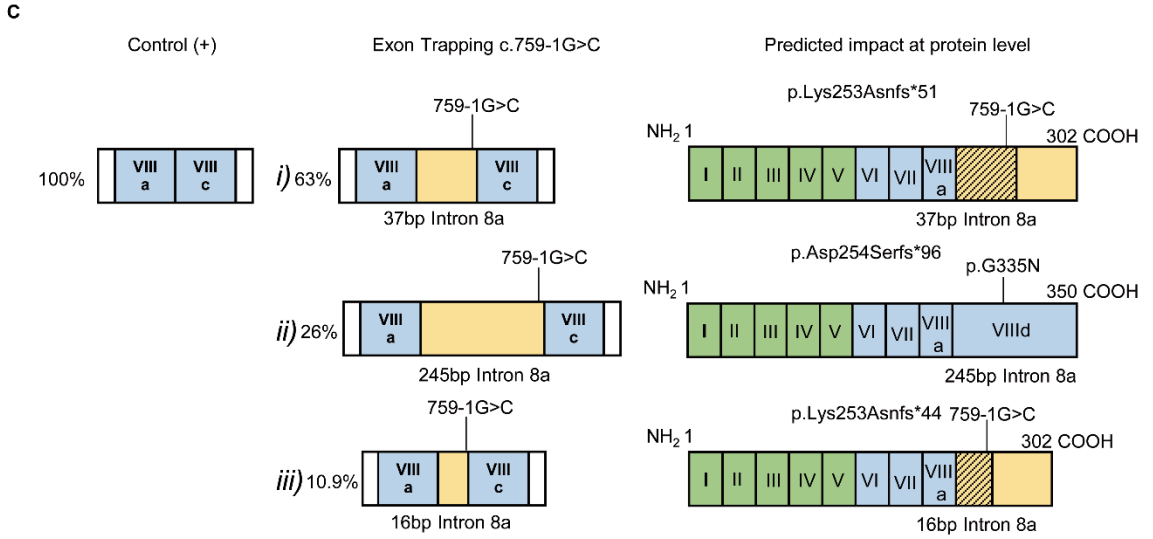
C
Control (+)
Exon Trapping c.759-1G>C
Predicted impact at protein level
100%
VIII a VIII c
i) 63%
759-1G>C
VIII a VIII c
37bp Intron 8a
p.Lys253Asnfs*51
759-1G>C
NH2 1
302 COOH
I II III IV V VI VII VIII a
37bp Intron 8a
ii) 26%
759-1G>C
VIII a VIII c
245bp Intron 8a
p.Asp254Serfs*96
p.G335N
NH2 1
350 COOH
I II III IV V VI VII VIII a VIIId
245bp Intron 8a
iii) 10.9%
759-1G>C
VIII a VIII c
16bp Intron 8a
p.Lys253Asnfs*44 759-1G>C
NH2 1
302 COOH
I II III IV V VI VII VIII a
16bp Intron 8a

Supplemental figure 2

mRNA analysis of *NCF4* mutants. (A) Quantitative PCR of the *NCF4* cDNA from EBV-B cells and neutrophils from patients carrying bi-allelic mutations of the *NCF4* gene. Data represent mean ± SEM. **(B)** Schematic diagram and proportional expression of different splice variants in cells from homozygous carriers of the c.118-1G>A and c.120_134del mutations. **(C)** Different spliced products and their frequency on overexpression of the WT sequence and of the sequence containing the c.759-1G>C mutation in an exon trapping experiment.

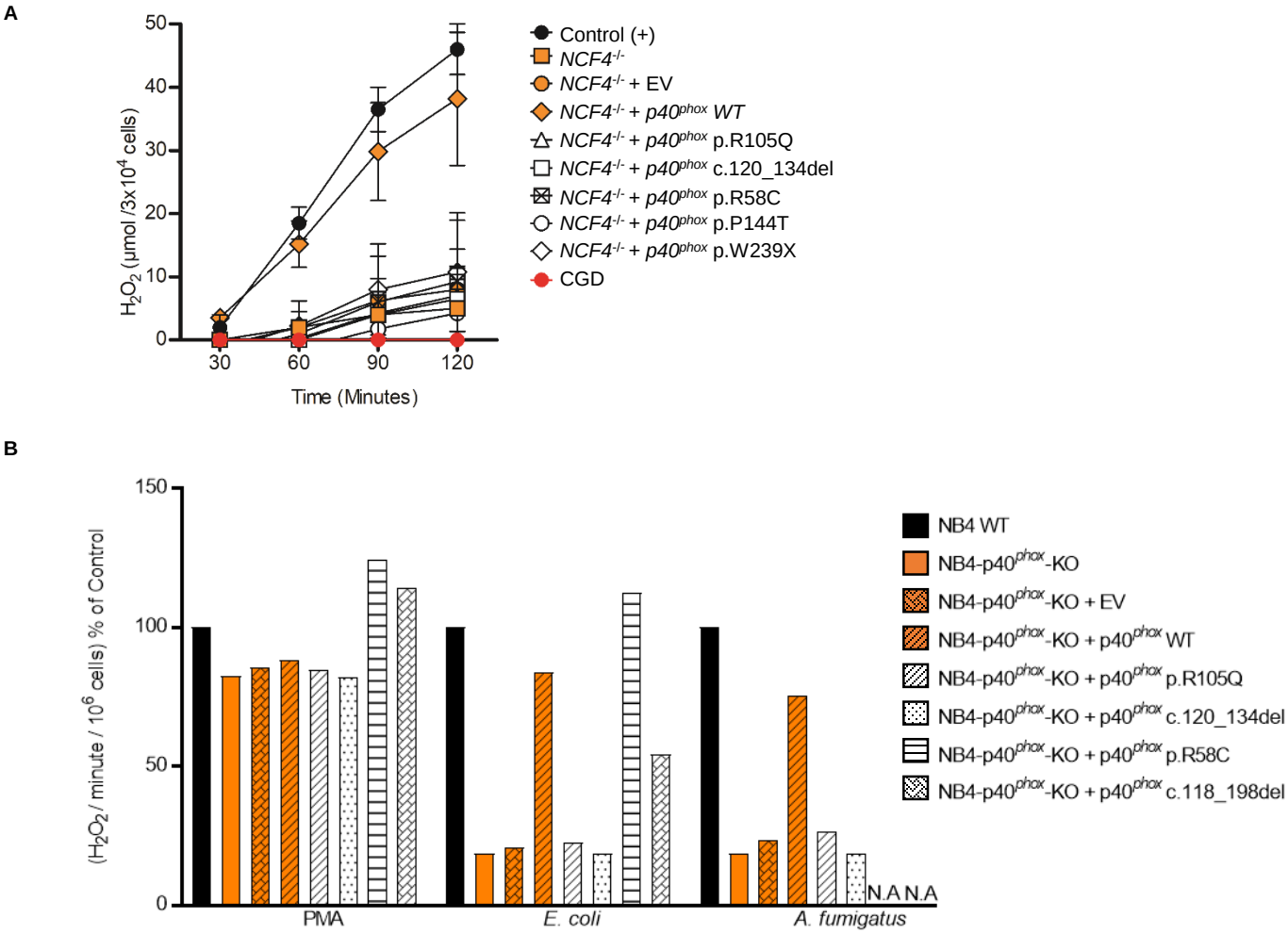

Supplemental figure 3

H_2O_2 release in transduced cells. (A) Kinetic of EBV-B cells stimulated with PMA. Experiment representative of three replicates. Data represent mean ± SEM. **(B)** Extracellular H_2O_2 generation by NB4 p40^{phox} knockout (KO) cells lines upon stimulation with PMA, *E. coli* and *A. fumigatus*. N=2-3. 2-Tailed Mann U Whitney test. Data represent mean ± SEM.

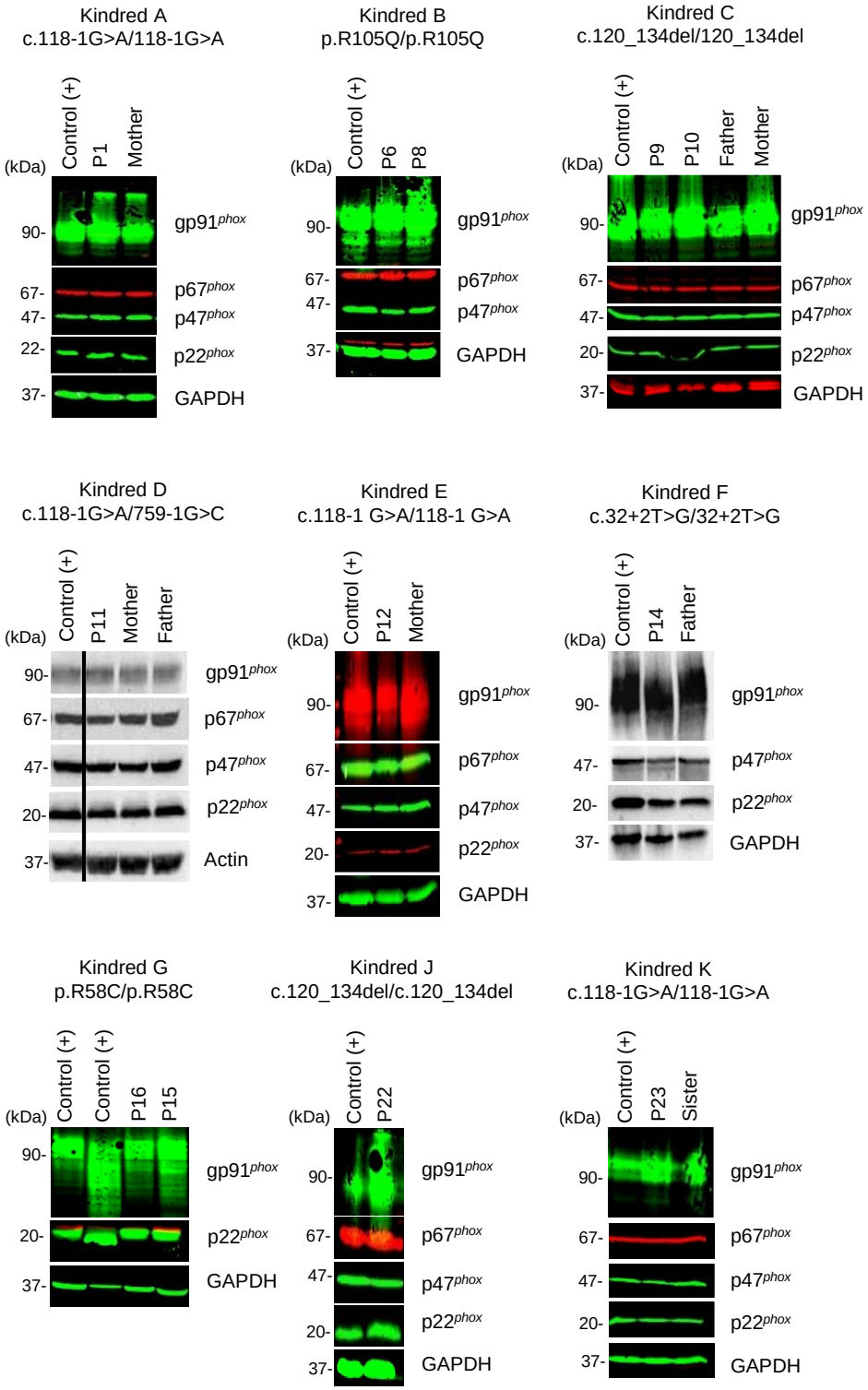

Supplemental figure 4

NADPH oxidase component expression in p40*phox*-deficient neutrophils. Western blot of total protein extracts from neutrophils of healthy controls, p40*phox*-deficient patients and heterozygous parents. Antibodies against gp91*phox*, p22*phox*, p67*phox* and p47*phox* were used. Actin or GAPDH protein was used as the loading control.

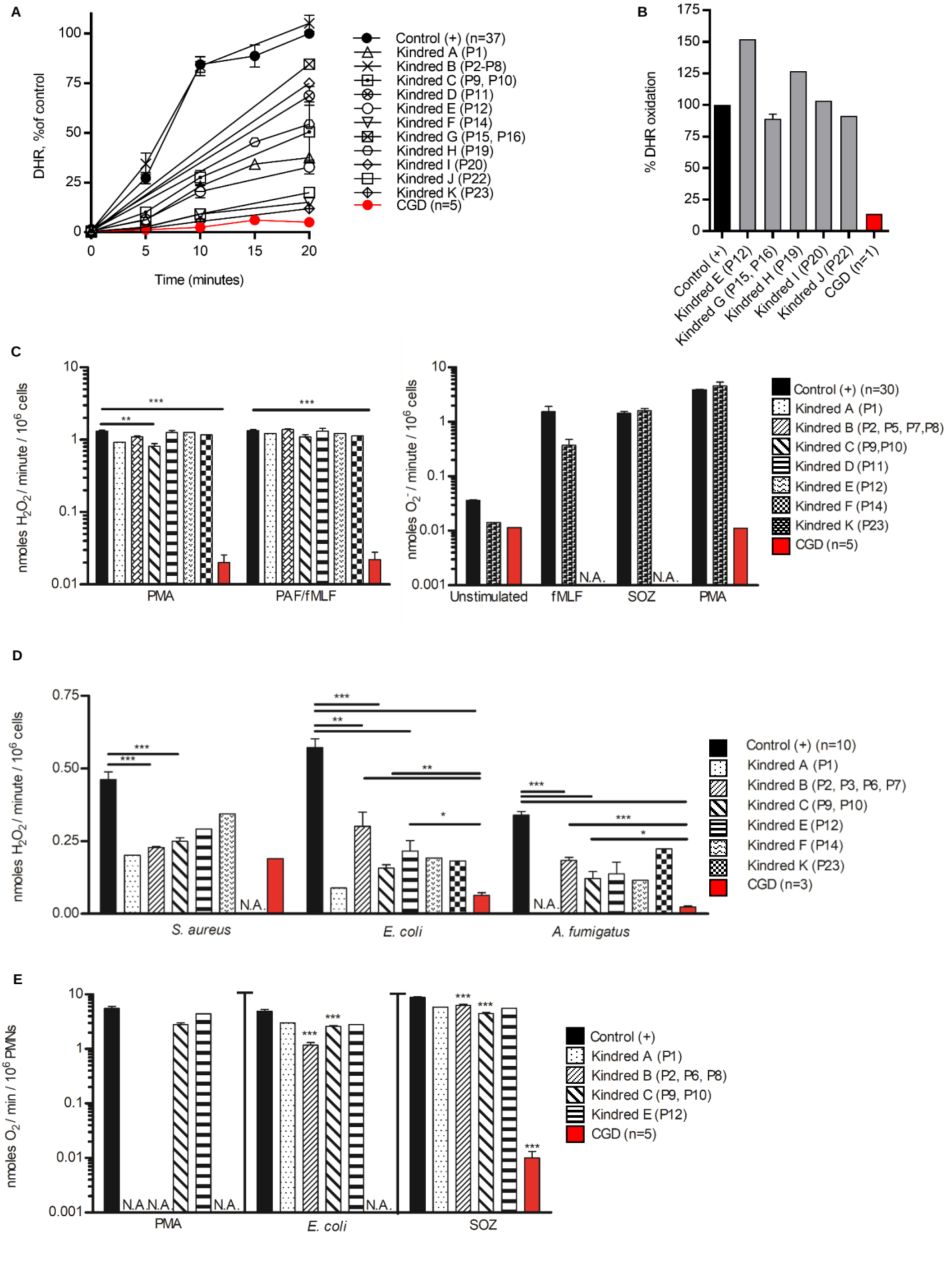
A
DHR, %of control
Time (minutes)
Control (+) (n=37)
Kindred A (P1)
Kindred B (P2-P8)
Kindred C (P9, P10)
Kindred D (P11)
Kindred E (P12)
Kindred F (P14)
Kindred G (P15, P16)
Kindred H (P19)
Kindred I (P20)
Kindred J (P22)
Kindred K (P23)
CGD (n=5)
B
% DHR oxidation
Control (+)
Kindred E (P12)
Kindred G (P15, P16)
Kindred H (P19)
Kindred I (P20)
Kindred J (P22)
CGD (n=1)
C
nmoles H2O2/ minute / 10^6 cells
PMA
PAF/fMLF
nmoles O2- / minute / 10^6 cells
Unstimulated
fMLF
SOZ
PMA
N.A.
Control (+) (n=30)
Kindred A (P1)
Kindred B (P2, P5, P7,P8)
Kindred C (P9,P10)
Kindred D (P11)
Kindred E (P12)
Kindred F (P14)
Kindred K (P23)
CGD (n=5)
D
nmoles H2O2/ minute / 10^6 cells
S. aureus
E. coli
A. fumigatus
Control (+) (n=10)
Kindred A (P1)
Kindred B (P2, P3, P6, P7)
Kindred C (P9, P10)
Kindred E (P12)
Kindred F (P14)
Kindred K (P23)
CGD (n=3)
E
nmoles O2/ min / 10^6 PMNs
PMA
E. coli
SOZ
Control (+)
Kindred A (P1)
Kindred B (P2, P6, P8)
Kindred C (P9, P10)
Kindred E (P12)
CGD (n=5)

Supplementary figure 5.

NADPH oxidase activity in p40^{phox}-deficient neutrophils and monocytes. (A) Kinetic of DHR oxidation upon PMA stimulation in neutrophils from healthy controls (*n=37*), p40^{phox}-deficient patients and a CGD patient. **(B)** Intracellular ROS production by DHR oxidation in monocytes from healthy controls, p40^{phox}-deficient patients and a CGD patient upon stimulation with PMA (400 ng/µL). **(C)** Extracellular H_2O_2 detection (left) in neutrophils from healthy controls (*n*=30), p40^{phox}-deficient patients (*n*=10) and CGD patients (*n*=5) upon stimulation with PMA, or PAF/fMLF. Extracellular O_2^- generation (right) by neutrophils from healthy controls (*n*=6), P11 (*n*=3) and a CGD patient (*n*=1) upon stimulation with fMLF, SOZ or PMA. **(D)** Extracellular H_2O_2 production by neutrophils from healthy controls (*n*=10), p40^{phox}-deficient patients (*n*=10) and CGD patients (*n*=3) upon stimulation with *E. coli, S. aureus* and *A. fumigatus*. N.A., not analyzed. **(E)** Oxygen consumption by neutrophils after stimulation with PMA, *E. coli* or SOZ. Healthy controls (*n*=3) and p40^{phox}-deficient patients (*n*=7) were tested with PMA; healthy controls (*n*=8) and p40^{phox}-deficient patients (*n*=13) were tested with *E. coli*; and healthy controls (*n*=13), p40^{phox}-deficient patients (*n*=11) and CGD patients (*n*=5) were tested with SOZ. Data represent mean ± SEM when *N*>3. N.A., not analyzed. *****p<0.05**,** **p<0.01 and ***p<0.001. For figures **(C)** and **(E)** the Bonferroni correction for multiple comparisons was applied and an adjusted p value of 0.0083 (*S. aureus* and *A. fumigatus*) or 0.0071 (*E. coli*, PMA, PAF/fMLF) was considered significant (*)**.**

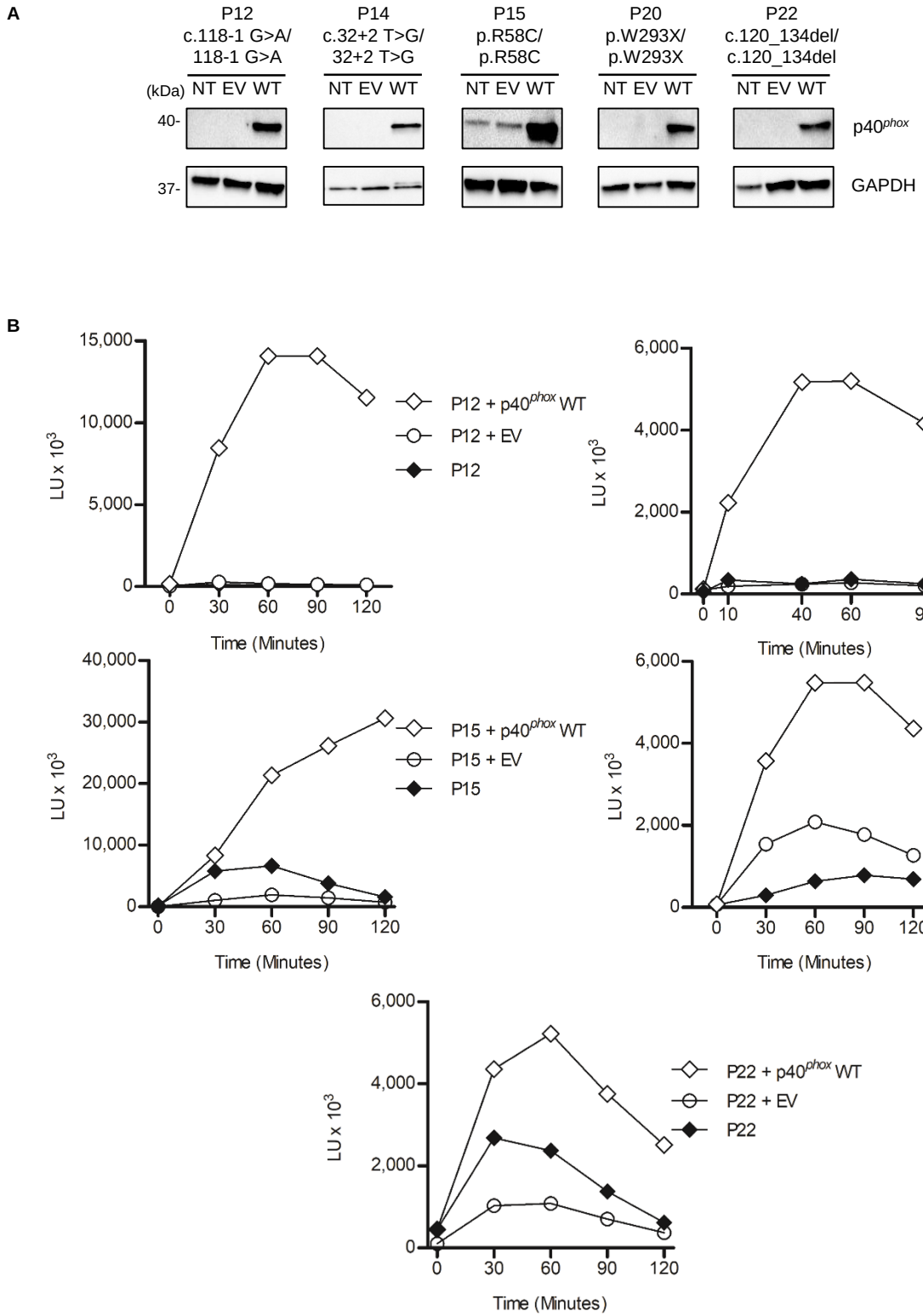

Supplementary figure 6.

Reconstitution of p40*phox* in EBV-B cells from patients. (A) p40*phox* protein expression of EBV-B cells transduced with an empty vector (EV) or a vector encoding the WT p40*phox* protein, and non-transduced cells, from P12, P14, P15 and P22. **(B)** Production of O_2^- upon PMA stimulation in p40*phox* deficient EBV-B cells transduced with EV or a vector encoding WT p40*phox* protein and non-transduced cells, from P12, P14, P15 and P22.

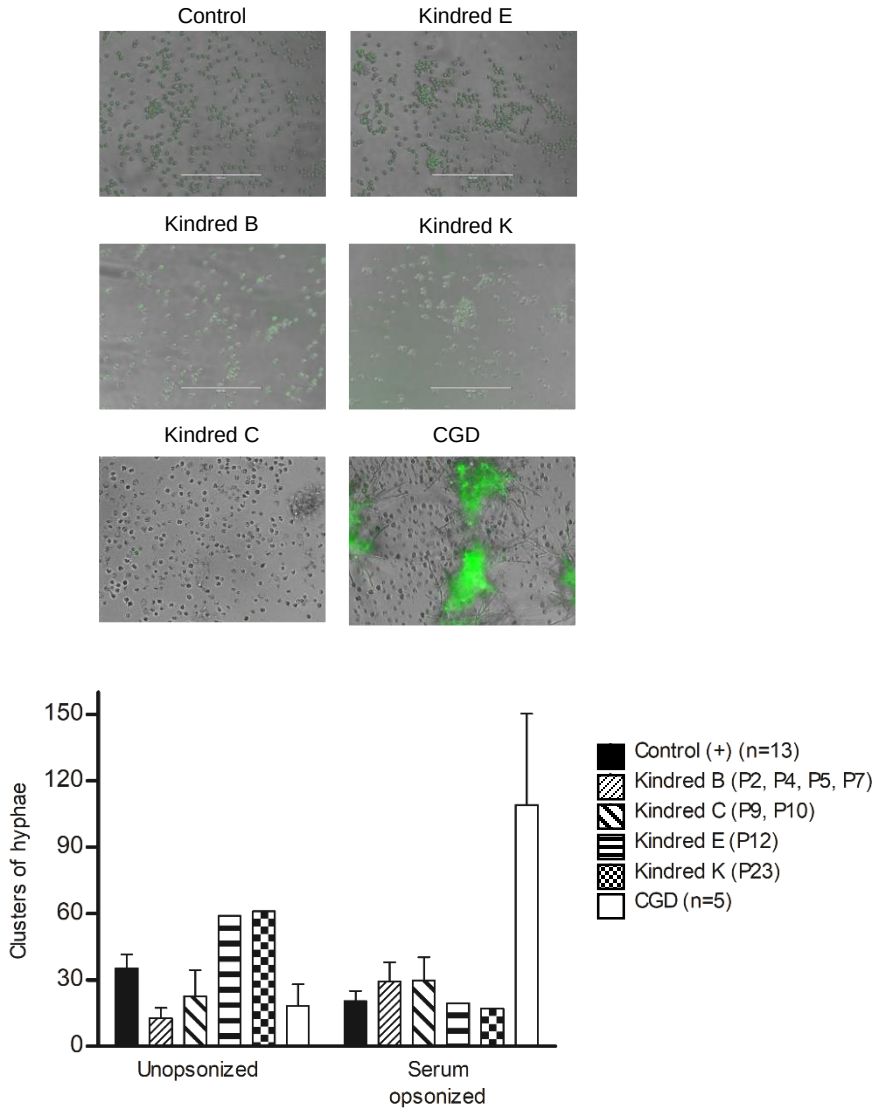

Supplementary figure 7.

Inhibition of *C. albicans* germination by neutrophils. Cocultures of *C. albicans* and neutrophils from healthy controls (*n*=13), p40^{phox}-deficient patients (*n*=8) and CGD patients (*n*=5). Inhibition of hypha formation was evaluated by microscopy. Upper panel: representative micrographs of incubations. Bottom panel: Quantification of hypha formation. Two-tailed Mann U Whitney test. Data represent mean + SEM when N≥3 or mean only when N<3. The Bonferroni correction for multiple comparisons was applied and an adjusted p value of 0.01 considered significant (*) and *** p<0.001.

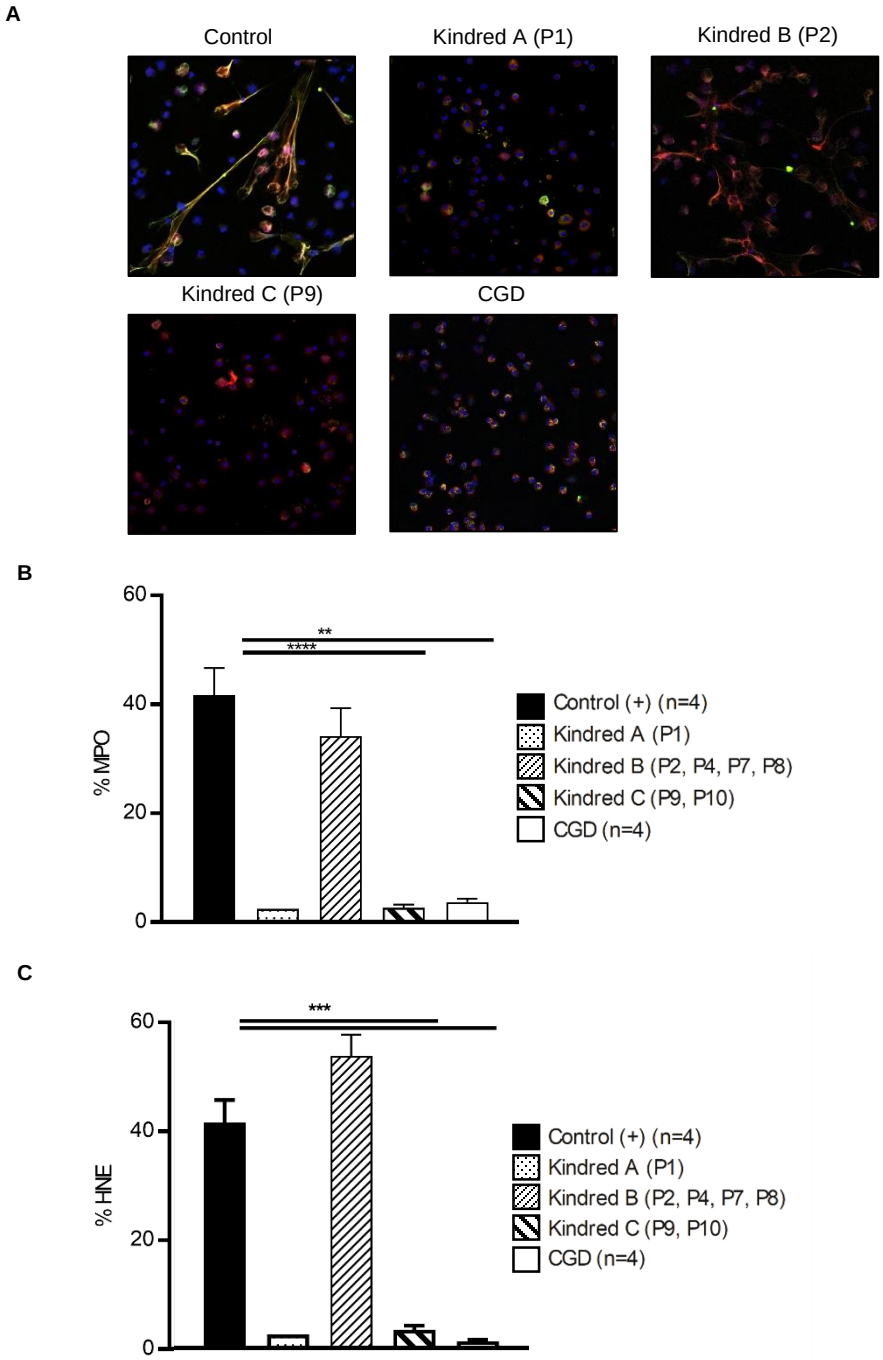

Supplementary figure 8.

Extracellular trap formation by neutrophils. **(A)** NET formation induced with PMA in neutrophils. The pictures are representative from healthy controls (*n*=4), p40^{phox}-deficient patients (*n*=7) and CGD patients (*n*=4). Original pictures after NET induction and staining for myeloperoxidase - MPO (red), human neutrophil elastase - HNE (green) and DNA (blue). NET quantification was performed as described in the Supplementary Methods. Relative MPO **(B)** and HNE **(C)** positive areas were measured by fluorescence microscopy. 4 Dots represent 4 fields analyzed during a single experiment. 2-Tailed Mann U Whitney test. Data represent mean + SEM when N≥3 or mean only when N<3. The Bonferroni correction for multiple comparisons was applied and an adjusted p value of 0.0125 was considered significant (*). *** p<0.001.

Supplementary Table 1. Comparison of clinical manifestations between patients with p40^{phox} deficiency and CGD cohorts

	USA cohort (ref. 7)	**European cohort** (ref. 9)	**Latin American cohort** (ref. 8)	**p40^{phox} deficiency study cohort**	
Frequency	% of patients ≥ 1 episode	% of patients ≥ 1 episode	% of patients ≥ 1 episode	% of patients ≥ 1 episode Total *n*=24	% of patients ≥ 1 episode Symptomatic *n*=20
Infections					
Lung	79%	66% (infection/inflammation not specified)	78%	13%	15%
Skin	5% cellulitis; 42% subcutaneous abscesses	17% abscesses; 17% dermatitis, 5% furunculosis, 6% BCG-itis	43%	42%	50%
Lymph node	53%	50%	60%	17%	20%
Liver	27% (hepatic abscesses)	32%	Not reported/specified	Absent	Absent
Urinary tract	Not reported	22%	22.5%	Absent	Absent
Bacteremia/ septicemia	18%	20%	25%	Absent	Absent
Widespread infection	Not reported/specified	Not reported/specified	Not reported/specified	4% (histoplasmosis)	5% (histoplasmosis)
Ear	Not reported	14%	30%	Absent	Absent
Bone	25%	13%	18%	Absent	Absent
Eye	Not reported/specified	11%	Not reported/specified	Absent	Absent
Brain	4% meningitis; 3% brain abscesses	7%	Not reported/specified	4%	5%

Autoimmunity/Hyper-inflammation					
Lung	16%	Not reported/specified	Not reported/specified	9%	11%
Skin	10%	2%	Not reported/specified	42%	50%
GI - oral	Not reported/specified	11% aphthae, 11% stomatitis, 11% gingivitis/caries	Not reported/specified	30%	37%
GI – (entero)colitis	17%	9%	Not reported/specified	25%	30%
GI – peri-anal	Not reported/specified	21%	Not reported/specified	17%	20%
Other	17%	Not reported/specified		13%	15.8%

GI: gastrointestinal

Supplementary Table 2. Comparison of genetic and genotypic characteristics in p40^{phox} deficiency and CGD (several different cohorts)

Characteristic	USA cohort (ref. 7)		European cohort (ref. 9)		Turkish cohort (ref. 19)		Latin American cohort (ref. 8)		Israeli cohort (ref. 18)		p40^{phox} deficient study cohort
Genetic type; frequency	XR = 259*	AR = 81*	XR = 279**	AR = 136**	XR = 34^	AR = 50^	XR = 53	AR = 18^^	XR = 32	AR = 52	p40^{phox} N= 24
Age at disease onset (years)	Not reported	Not reported	Not reported	Not reported	Not reported	Not reported	1.8 (0-13)	2.8 (0-7)	0.9 (0-4)	3.5 (0-4)	6 (1-17)
Age at diagnosis (years)	3.0	7.8	4.9	8.8	2.7 (0-8)	5.2 (0-18)	3.6 (0-17)	8.2 (0-14)	3.2 (0-8)	7.0 (0-40)	13.9 (1-46)
Mortality	21%	9%	23%	15%	9%	12%	Not reported	Not reported	22%	17%	0%
NADPH oxidase activity (neutrophils)	Not reported	Not reported	Not reported	Not reported	DHR	DHR	Not reported	Not reported	DHR	DHR	DHR (PMA)
Absent	Not reported	Not reported	Not reported	Not reported	100%	0%	Not reported	Not reported	90%	0%	0%
Residual	Not reported	Not reported	Not reported	Not reported	<2% of control	p47^{phox} 8.5% p22^{phox} <2% p67^{phox} <2% of control	Not reported	Not reported	10% with 41% normal values	p47^{phox} 5.4% p22^{phox} 10% p67^{phox} 4% of control	100% with 50-90% of control values (400ng/mL of PMA)

* *N*=28 unknown ** *N*=37 unknown ^*N*=5 unknown ^^including 16 with p47^{phox} deficiency

Supplementary Table 3. Primer sequences and conditions for genomic amplification of *NCF4* gene.

Primer sequence	Conditions
Exon 1	We used Rapid Cycler technology (BioFire Diagnostics, USA) with 50 cycles of 5 s at 95°C, 30 s at 65°C and 60 s at 72°C, in 15 µl of PCR buffer containing 2 IU of Taq polymerase (Promega Benelux, The Netherlands), 2 U TaqStart antibody (Takara, USA), 50 ng of each primer, 200 µM for each of the dNTPs, 50 mM KCl, 1.5 mM MgCl2, 0.1% (v/v) Triton X-100, 10 mM Tris, pH 9.0 at 25°C, in 10-µl glass capillaries (BioFire Diagnostics).
5'TGAGGCTTGGCGCCAAGGACTGACA-3'	
5'-CCCTAAGGCCCTATGAGGAGCAGTG-3'	
Exon 3	
5'-ACCTCTTTTTGGCTTGTGCTCCTGG-3'	
5'-GGGGGCCCTGGAAGGAAGGAGAGTCA-3'	
Exon 4	
5'-TCTGGCCAGGGTTCCTGGCCTGTAG-3'	
5'-GTACGTGGGCTCCCCCACCAATACT-3'	
Exon 2	
5'-GCACTCTACCTCATACCCGG-3'	2.5mM of magnesium and 10% of DMSO TM= 59°C
5'-TCAGAGGGCAAGGTTCAGAG-3'	
Exon 6	
5'-CCCCTCTTCTCTCTCCACAG-3'	2.5mM of magnesium and 10% of DMSO TM= 59°C
5'-GCTGTAACCCCTTCCTTCCT-3'	
Exon 7	
5'-TTACTGCACGCTTCTCCTCA-3'	2.5mM of magnesium and 10% of DMSO TM= 59°C
5'-TTCCCTCCAACCTCACCTTC-3'	
Exon 8	
5'-TCCCTTCTCTTCCTCTGCAG-3'	2.5mM of magnesium and 10% of DMSO TM= 61°C
5'-GTATCTAACTCCCCAGCCCC-3'	

Supplementary Table 4. Reference and clones of antibodies.

Antibody	Source	Catalogue Number	Clone Number
anti-gp91^{phox}	Sanquin Reagents, Netherlands	MW1842	48
anti-gp91$_{phox}$ (Intracellular Stainig)	Santa Cruz Biotechnology, USA	sc-130543	54.1
anti-p22^{phox}	Sanquin Reagents, Netherlands	MW1843	449
anti-p22^{phox} (Intracellular Stainig)	Santa Cruz Biotechnology, USA	sc-130550	44.1
anti-p47^{phox}	Santa Cruz Biotechnology, USA	sc-17845	D-10
anti-p47^{phox}	Merck Millipore, USA	07-001	Rabbit antiserum. LOT: DAM1413939
anti-p47^{phox} (Intracellular Stainig)	Santa Cruz Biotechnology, USA	sc-17845	D-10
anti-p67^{phox}	Merck Millipore, USA	07-002	polyclonal
anti-p67^{phox} (Intracellular Stainig)	Santa Cruz Biotechnology, USA	sc-374510	D-6
anti-p40^{phox}	Abcam, UK	ab76158	EP2142Y
anti-p40^{phox}	Merck Millipore, USA	07-503	Rabbit polyclonal. LOT: 2876659
Anti-GAPDH	Merck Millipore, USA	MAB374	6C5
The anti-p22^{phox}, anti-p47^{phox}, anti-p67^{phox} and anti-gp91^{phox}	Produced by dr. Thomas L. Leto, NIH	Produced by Dr. Thomas L. Leto, NIH	polyclonal
anti-actin	Merck Millipore, USA	MAB1501	C4
Secondary antibodies			

Donkey-antigoat-IgG IRDye 800CW	LI-COR Biosciences, USA	629-68023	polyclonal
goat anti-mouse-IgG IRDye 800CW	LI-COR Biosciences, USA	926-68070	polyclonal
goat anti–rabbit-IgG IRDye 680CW	Life technologies, USA	A11070	polyclonal
Goat anti-rabbit IgG (H+L)-HRP conjugate	Bio-rad, USA	170-6515	polyclonal
Goat anti-mouse IgG (H+L)-HRP conjugate	Bio-rad, USA	170-6516	polyclonal

Supplementary Methods

Neutrophil purification

Neutrophils were purified by centrifuging blood on a Percoll gradient with a density of 1.074 g/ml (purity >95%). The erythrocytes in the pellet were lysed with isotonic NH_4Cl-$KHCO_3$-EDTA solution (1). Cells were resuspended in $HEPES^+$ incubation medium.

Phagocytosis

Zymosan (10 mg/ml, Sigma-Aldrich, St. Louis, MO, USA), *E. coli* (OD_{600} 1.0, strain ML-35) and *S. aureus* (OD_{600} 1.0, strain Oxford) were incubated with 1 µg of FITC (Sigma-Aldrich) for 30 minutes at 37°C, resuspended in PBS and opsonized with 10% (v/v) serum for 10 minutes at 37°C at 550 rpm (Eppendorf Thermomixer C, Eppendorf AD, Hamburg, Germany). The opsonized zymosan was added to $0.5x10^6$ neutrophils and 125 µl of HEPES+. Samples were removed at various time points and mixed with STOP-buffer (20 mM NaF, 0.5 % [w/v] PFA, 1% [v/v] BSA in PBS) in a 96-well Maxisorp plate, on ice (Thermo Fisher, Roskilde, Denmark). Phagocytosis was analyzed by assessing the percent FITC-positive cells and the mean MFI, by flow cytometry (FACSCANTO II/LSR).

Degranulation

Protease release after degranulation was measured by assessing the degradation of fluorescent DQ-green BSA (bovine serum albumin) (Life Technologies), as previously described (2). In short, neutrophils ($2x10^6$/ml) were incubated with DQ-BSA (1:90) and PAF (1 µM) or cytochalasin B (5 µg/ml) for 5 min at 37°C. The cells were then stimulated with 1 µM fMLF or 100 ng/ml PMA (all stimuli were purchased from Sigma-Aldrich, St. Louis, MO, USA). An

unstimulated control value and a 100% content value with Triton X-100 (1% w/v) were also determined. Degranulation was assessed with the Infinite F200-pro plate reader (Tecan).

Bacterial and fungal killing

The killing of bacteria by neutrophils was determined as previously described (3). Briefly, *S. aureus* and *E. coli* were grown aerobically at 37°C in Luria Bertani (LB) broth for 3 hours. Pathogen density was then adjusted to an OD_{600} of 1.0 in PBS and the pathogens were opsonized with 10% (v/v) pooled human serum at 37°C for 15 minutes before incubation with $2x10^6$ neutrophils at a bacterium/neutrophil ratio of 5:1. At various time points, 50-µl samples were added to 2.5 ml of H_2O/NaOH pH 11, and the samples were then spread onto LB agar plates for overnight incubation. CFUs were counted the following day. For *S. aureus* killing by NB4 cells, $10x10^6$ cells/ml were initially incubated overnight with IFN-γ (1:4000) and G-CSF (1:2000, both from PeproTech, Rocky Hill) . The cells were then used with a yeast/neutrophil ratio of 10:1.

C. albicans conidia were grown at 30°C, and used at an OD_{625} of 0.2. The inhibition of *C. albicans* germination and hyphenation was analyzed as previously described (4). In brief, GFP-*C. albicans* conidia were incubated with neutrophils overnight at 37°C, under an atmosphere containing 5% CO_2. The next day, clusters of *Candida* hyphae were counted under a digital fluorescence microscope (Evos, Belgium). Both *Candida* killing assays were performed with serum-opsonized and non-opsonized yeasts at a yeast/neutrophil ratio of 4:1. The killing of *A. fumigatus* hyphae was assessed as previously described (5).

Western blotting of phagocyte proteins

The presence of the various phagocyte NADPH oxidase proteins was analyzed by western blotting. Reference number and clones are listed in Supplementary Table 4. In neutrophils from kindreds A, B, C, E, G, J and K monoclonal antibodies anti-gp91^{phox} and anti-p22^{phox} were used. Monoclonal anti-p47^{phox}, polyclonal anti-p67^{phox} and monoclonal anti-p40^{phox} antibodies were used. Anti-GAPDH antibodies was used for detection of the loading control. For analyses of protein content in kindred D, a monoclonal rabbit anti-p40^{phox} antibody was used. The anti-p22^{phox}, anti-p47^{phox}, anti-p67^{phox} and anti-gp91^{phox} antibodies were provided by Dr. Tom Leto, NIAID, NIH. Actin was used as a loading control. For p40^{phox} expression in neutrophils from the patients of kindreds F, G and I and in monocyte-derived macrophages from patients of kindreds E, I and J, polyclonal anti-p40^{phox} antibodies were used. Anti-GAPDH antibody was used for detection of the loading control. The secondary antibodies used were donkey-anti-goat-IgG IRDye 800CW, goat anti-mouse-IgG IRDye 800CW or goat anti–rabbit-IgG IRDye 680CW Antibody binding was quantified on an Odyssey Infrared Imaging system (LI-COR Biosciences, USA).

Extracellular O_2^-: cytochrome *c* reduction

Extracellular O_2^- production was assayed by evaluating cytochrome-*c* reduction. Neutrophils ($1x10^6$/ml) were incubated at 37°C with ferri-cytochrome *c* (100 µM), after which we added buffer, fMLF (10^{-7} M), serum-opsonized zymosan (SOZ); Zymosan, (Sigma-Aldrich, USA) 1.0 mg/ml, opsonized with 10% v/v pooled serum for 10 minutes at 37°C), or PMA (100 ng/ml). The supernatant was analyzed spectrophotometrically to determine the O_2^--dependent reduction of ferri-cytochrome *c* at 549.5 nm. Superoxide dismutase was added to a reaction tube prepared in an identical manner, to serve as a blank.

Intracellular oxidase activity: luminol-enhanced chemiluminescence

Neutrophils were assessed for intracellular ROS production by evaluating chemiluminescence. Neutrophils (100,000 cells/well) in 200 µl of Hank's Balanced Salt Solution (HBSS) with divalent cations and 10 mM HEPES medium were incubated with 100 µM luminol at 37°C for 10 minutes. Soluble and particulate ligands, buffer, PMA (100 ng/ml), SOZ (0.1 mg/ml), and heat-killed *E. coli* (100:1 neutrophil) were added to the wells. Light production was monitored every 2 min for 120 min on a Promega Glomax (Promega Corp., USA) luminescence plate reader.

Overall oxidase activity: oxygen consumption

Oxygen concentration was measured with a Clark electrode at 37°C, with stirring, as previously described (6). Neutrophils ($2.5x10^6$/ml) were stimulated with SOZ (1 mg/ml), *E. coli* (OD_{600}= 0.1 in the presence of 2 mM azide) or PMA 100 ng/ml.

Expression of *NCF4* mutations in transfected HEK293T cells

Direct mutagenesis was performed to obtain the different *NCF4* mutations in the PCMV6-*NCF4*-WT-DDK plasmid from Origene. Cells were transfected with 2 µg of plasmid in the presence of Lipofectamine (Invitrogen) for 24 hours. The overproduced $p40^{phox}$ protein was detected in total extracts by western blotting with a polyclonal anti-$p40^{phox}$ antibody from Merck Millipore and an anti-DDK antibody from Origene.

Generation of EBV-B cells and retrovirus-mediated transduction with *NCF4* alleles in **EBV-B cells**

EBV-B cells were cultured in RPMI medium supplemented with 10% (v/v) FCS (referred to here as complete medium). The presence of p40^{phox} was analyzed by western blotting. Monoclonal anti-gp91^{phox}, anti--p22^{phox} and anti-GAPDH (loading control) antibodies were obtained from Santa Cruz. Polyclonal anti-p47^{phox} , anti-p22^{phox} and anti-p40^{phox} antibodies were obtained from Merck Millipore. Retrovirus-mediated transduction was performed as previously described (7). Briefly, the coding sequences of the WT and mutant *NCF4* alleles were inserted into the pLZRS-IRES-ΔNGFR plasmid. The new plasmids generated were used to transfect Phoenix cells for virus production. EBV-B cells from p40^{phox}-deficient patients were infected with the viral concentrate. Stable retrovirus-mediated transduction was confirmed in cells expressing CD271, which were then used for functional assays.

Viral transduction of NB4 KO cell lines.

The coding sequence of p40^{phox} (NM_000631) without a stop codon was ordered from Invitrogen, with a 5' flanking sequence of GAATTCCGCCACC and a 3' flanking sequence of GGGTCGAC. Several mutations not affecting protein coding were also introduced into the target sequence of the CRISP oligomers. The R105Q mutant was created with the QuikChange Site-Directed Mutagenesis Kit (Agilent Technologies, USA). The p40^{phox} sequence was inserted into pmCherry-N1. The p40^{phox}-mCherry fragment from this construct was digested with *Eco*RI and *Not*I and inserted into pENTR1A. The resulting pENTR1A - p40^{phox}-mCherry construct was recombined, in the presence of LR Clonase II (Thermo Fisher Scientific, USA) with pRRL PPT SFFV GFP prester SIN, in which the GFP was replaced with a Gateway Cassette. The resulting plasmid, pSIN – p40^{phox}-mCherry, was used to reconstitute the knockout cell line. NB4 p40^{phox} KO cells were reconstituted by lentiviral transduction. Lentiviral particles were generated by the transient cotransfection of HEK293T cells with pSIN – p40^{phox}-mCherry, pMDLgp, pRSV-rev and

pCMV-VSVg, with TransIT-LT1. The day after transfection, the cells were plated on NB4 medium. The virus-containing supernatant was harvested on days 2 and 3 after transfection and filtered through 0.45-μm pores; we then used 1 ml of the filtrate with $5x10^5$ NB4 $p40^{phox}$ KO cells on two successive days. Cells positive for mCherry were selected by FACS sorting. For differentiation, NB4 cells were grown at a density of $5x10^5$ cells/ml, and all-*trans* retinoic acid (ATRA) was added to a final concentration of 5 μM. One volume of medium was added to the cells between three and five days after the addition of ATRA.

Neutrophil extracellular trap (NET) formation

We incubated 250,000 neutrophils on coverslips (12 mm, Menzel GmbH & Co KG, Braunschweig, Germany) in a sterile 24-well plate (Nuclon Delta Surface, Thermo Fisher) at 37°C, under an atmosphere containing 5% CO_2, for 10 minutes, after which PMA (100 ng/ml) was added. The cells were then incubated for 3 hours at 37°C (5 hours for NB4 cells), under an atmosphere containing 5% CO_2. Cells were fixed by incubation with 3.7% (w/v) paraformaldehyde (PFA) in PBS. After overnight storage at 4°C, the cells were incubated with mouse anti-myeloperoxidase (MPO) (Abcam, Cambridge, UK) and rabbit anti-human elastase (HNE) (Sanquin) antibodies diluted 1:500 in PBS/5% (v/v) BSA, for 30 minutes at room temperature. The NET components MPO, HNE and DNA were stained red, green and blue, respectively, with anti-mouse secondary antibodies (goat anti-mouse-IgG 680 RD, 926-68070, Li-Cor, Bad Homburg, Germany), anti-rabbit secondary antibodies (goat anti-rabbit-IgG 488, Life Technologies) 1:500, and Hoechst stain (Sigma-Aldrich; 1:40,000). NET formation was quantified by confocal microscopy (TCS SP8, Leica, Wetzlar, Germany) as previously described (8). We observed at least four fields of 2, 922 x 2,922 μm with a 40x objective lens. The same contrast was used for all images. Images from individual color channels (red for MPO, green for NE and blue for DNA) were exported to ImageJ

(NIH, Bethesda, MD, USA). Contrast was adjusted to minimize background autofluorescence, and the same fluorescence threshold was applied to all samples within the same experiment. The MPO- and HNE-stained areas were measured as the percentage of the image area covered by positive fluorescence staining per field, with ImageJ (NIH).

Exon trapping

PCR of genomic DNA flanking position c.759-1, including the entire exon 8a, intron 8a and exon 8c, was performed with gDNA from a healthy control. The PCR product was inserted into pSPLP3 for exon trapping. Targeting mutagenesis was performed to generate the c.759-1G>C mutation. COS 7 cells were transfected over a 24 h period with 500 ng of plasmid containing the WT or mutated sequence. RNA was obtained from the transfected cells and subjected to reverse transcription to generate cDNA. PCR was performed on the cDNA, with primers SD6 and SA2, which bind the sequencing flanking the artificial exon in pSPLP3, and the amplification of the spliced products was evaluated by sequencing one hundred colonies by TOPOTA amplification.

Supplementary references

1. Roos D, Loos JA. Changes in the carbohydrate metabolism of mitogenically stimulated human peripheral lymphocytes. I. Stimulation by phytohaemagglutinin. *Biochim Biophys Acta.* 1970;222(3):565-582.
2. Kuijpers TW, et al. Combined immunodeficiency with severe inflammation and allergy caused by ARPC1B deficiency. *J Allergy Clin Immunol*. 2017 ;140(1):273-277.
3. Decleva E, Menegazzi R, Busetto S, Patriarca P, Dri P. Common methodology is inadequate for studies on the microbicidal activity of neutrophils. *J Leukoc Biol.* 2006;79(1):87-94.
4. Drewniak A, et al. Invasive fungal infection and impaired neutrophil killing in human CARD9 deficiency. *Blood.* 2013;121(13):2385-2392.
5. Gazendam RP, et al. Impaired killing of Candida albicans by granulocytes mobilized for transfusion purposes: a role for granule components. *Haematologica.* 2016;101(5):587-596.
6. Weening RS, Roos D, and Loos JA. Oxygen consumption of phagocytizing cells in human leukocyte and granulocyte preparations: a comparative study. *J Lab Clin Med.* 1974;83(4):570-7.

7. Martinez-Barricarte R, et al. Transduction of Herpesvirus saimiri-transformed T cells with exogenous genes of interest. *Curr Protocol Immunol.* 2016;115(7.21c.1-7.c.12.

8. McDonald B, Urrutia R, Yipp BG, Jenne CN, and Kubes P. Intravascular neutrophil extracellular traps capture bacteria from the bloodstream during sepsis. *Cell Host Microbe.* 2012;12(3):324-33.